



Experimental studies on passive inclined solar panel absorber solar still

C. Sasikumar¹ · A. Muthu Manokar² · M. Vimala³ · D. Prince Winston⁴ · A. E. Kabeel⁵ · Ravishankar Sathyamurthy^{5,6}  · Ali J. Chamkha⁷

Received: 29 January 2019 / Accepted: 30 August 2019 / Published online: 11 September 2019
© Akadémiai Kiadó, Budapest, Hungary 2019

Abstract

This manuscript aims to analyze the passive inclined solar panel basin (PISPB) still at diversified flow rate of water (m_f). The freshwater collected from the solar still for different m_f at 4.68, 7.56 and 10.08 kg h⁻¹ is 3.7, 2.7 and 1.6 kg, respectively. Results showed that at higher flow condition, the still energy and exergy efficiency decreases and it is estimated as 36.06, 25.56 and 16.95% and 2.97, 1.91 and 1.01%, respectively, for flow rates of 4.68, 7.56 and 10.08 kg h⁻¹. Results revealed that electrical, thermal and exergy efficiency of photovoltaic panel increases under higher flow condition and it is found as 8.05, 8.81 and 9.44%, 11.43, 20.8 and 22.17 and 19.38, 20.58 and 21.16% for mass flow rates of (m_f) 4.68, 7.56 and 10.08 kg h⁻¹, respectively. When the m_f increases, there is a decrease in the PISPB still distilled water production rate, thermal and exergy efficiency, and there is an increase in power production, electrical, thermal and exergy efficiency through the photovoltaic panel.

Keywords Passive solar still · Mass flow rates · Enhancement · Electrical efficiency · Thermal efficiency

Abbreviations

CSS	Conventional solar still
CHTC	Convective heat transfer coefficient
EHTC	Evaporative heat transfer coefficient
ISPB	Inclined solar panel basin
PSS	Pyramid solar still
PV	Photovoltaic
SSS	Stepped solar still

List of symbols

A	Area (m ²)
h	Heat transfer coefficient (W m ⁻² K ⁻²)
I	Current (A)
$I(t)$	Solar intensity (W m ⁻²)
L	Latent heat of vaporization (kJ kg ⁻¹ K ⁻¹)
M	Hourly productivity from solar still (kg m ⁻² h ⁻¹)
P	Partial vapor pressure (N m ⁻²)
T	Temperature (°C)
V	Voltage (V)

✉ Ravishankar Sathyamurthy
raviannauniv23@gmail.com

¹ Department of Mechanical Engineering, Bannari Amman Institute of Technology, Sathyamangalam, Erode, Tamil Nadu, India

² Department of Mechanical Engineering, B.S. Abdur Rahman Crescent Institute of Science and Technology, Chennai, Tamil Nadu 600048, India

³ Department of Electrical and Electronics Engineering, R.M.K. Engineering College, Chennai 601 206, India

⁴ Department of Electrical and Electronics Engineering, Kamaraj College of Engineering and Technology, Virudhunagar 626001, India

⁵ Mechanical Power Engineering Department, Faculty of Engineering, Tanta University, Tanta, Egypt

⁶ Department of Automobile Engineering, Hindustan Institute of Technology and Science, Chennai, Tamil Nadu 603103, India

⁷ Mechanical Engineering Department, Prince Sultan Endowment for Energy and Environment, Prince Mohammad Bin Fahd University, Al-Khobar 31952, Saudi Arabia

η	Efficiency (%)
m_f	Mass flow rate of water
T_p	Panel temperature

Subscripts

a	Ambient
c	Convective
d	Daily
e	Evaporative
g	Glass
gi	Inner glass
pv	Photovoltaic
s	Surface area of condensing cover
w	Water

Introduction

A deficit in the amount of accessible potable water is a critical problem for several countries. Dearth conditions of groundwater, which contains harmful microorganisms and dissolved salts, require purification before being used. Hence, an interest in inventing new technologies to improve the freshwater source arises. Among the methods available, the solar still desalination technique serves the purpose effectively by utilizing the abundant natural resources such as sea water and sunlight. Especially in coastal areas, solar panel integrated solar still can be used as the best method to obtain freshwater as well as effectively generating power [1–24].

Agouz et al. [25] derived an inclined solar still (ISS) performance with a closed-loop continuous water flowing system. The main advantage of the closed-loop water flowing system over the open loop water flowing system is that it reduces the heat loss and hence improves the freshwater productivity. It was reported that ISS productivity and efficiency mainly depend on the m_f and wind velocity. Aybar [26] mathematically investigated the ISS performance by modifying the m_f and solar intensity. It was concluded that decreasing the m_f increases the water temperature. Maximum temperature of 49.19, 50.89 and 52.85 °C is obtained for the flow rate of 3.6, 5.4 and 7.2 kg h⁻¹, respectively, at the solar intensity of 700 W m⁻². Aybar et al. [27] carried out experiments on ISS by substituting the bare absorber plate with black-fleece wick and black-cloth material. This resulted in a 2–3 times higher production of freshwater using wick materials compared to the bare plate. Sharon et al. [28] modified the absorber plate of ISS with woolen wick and experimentally investigated the enhancement in freshwater production. The maximum productivity of 4.54 and 4.99 L day⁻¹ is

obtained for the wick-type and basin-type ISS, respectively. Multi-effect wick-type ISS was experimentally studied by the Yeh and Chen [29, 30]. The benefit of using multi-effect ISS is that it reduces the reflection of heat loss by absorbing solar intensity in more than one basin. Henceforth, the multi-effect ISS enhances the yield by using the latent heat. Sathyamurthy et al. [31] theoretically analyzed the novel baffle plate-attached ISS by changing the m_f and the temperature of feed water. The summarized result is that the maximum distillate production is 3.5 kg m⁻² day⁻¹ at the minimum m_f . Nagarajan et al. [32] comparatively examined the ISS with baffles and without baffles and submitted the maximum productivity of 5.5 and 3.5 kg m⁻² day, respectively. From the experimental results, it was found that there is a 37.04% increase in freshwater production by attaching the baffles in ISS over the normal ISS, and it revealed that increase in contact time between the basin and the saline water improves the freshwater production rate. El-Agouz [33] comparatively inspected the stepped solar still (SSS) and the conventional solar still (CSS) and stated that the SSS increases the freshwater production rate at about 43–48% more than the CSS. In the second modification, a cotton wick was incorporated in the SSS basin which escalated the yield increase by about 47–53% more than conventional-type solar still. Omara et al. [34] augmented the potable water produced by SSS with internal reflectors and recorded the maximum daily yield of 3720, 5840 and 6350 mL m⁻² day⁻¹ for the CSS, SSS and SSS with internal reflectors, respectively. The maximum increase in yield of 57% and 75% is obtained for the SSS and SSS with reflectors over the CSS. Omara et al. [35] also integrated external reflectors along with internal reflectors and reported that the proposed SSS give 125% higher output than the CSS. Multi-wick ISS was researched by Sodha et al. [36]. In their research work, blackened wet jute cloth is used to enhance the evaporation rate. In the ISS, shadowing effect was minimized because of small walls which in turn make it cost-effective compared to the CSS. Multi-wick ISS produced 34% overall efficiency and 2.5 L productivity. Sathyamurthy et al. [37] experimented a novel crescent-shaped absorber solar still with baffles by shifting the m_f and number of baffles and reported the yield of about 3 kg m⁻². The pyramid solar still (PSS) integrated with baffle-attached ISS was theoretically studied by Naveen Kumar et al. [38]. The maximum freshwater production of about 7.2 kg m⁻² is obtained for the still integration. Naveen Kumar et al. [39] and Panchal et al. [40] also researched the performance of triangular PSS, ISS and triangular PSS integrated with baffle-attached ISS. The research was carried out by varying the mass of water inside the PSS and maintaining the constant m_f in an ISS. The maximum productivity of about 7.52 kg m⁻² is

obtained for the still integration. Detailed reviews of the progress and designs of ISS [41, 42] were studied. From the detailed review, it is inferred that a lot of design modifications were carried out in the ISS. But far fewer experimental works were reported on a hybrid active ISS. The effect m_f in weir-type cascade solar still was experimentally studied by Farshad et al. [43]. The maximum yield from their study is about $7.4 \text{ kg m}^{-2} \text{ day}^{-1}$ at the minimum m_f . It was reported that m_f is inversely proportional to the yield of the system. Muthu Manokar et al. [44, 45] designed a novel ISPB still and experimentally studied the performance of the still by three different insulation conditions. It was concluded that the ISPB still with the sidewall and bottom insulation increases the panel temperature up to $66 \text{ }^\circ\text{C}$ which is 16.67% higher than the ISPB still with only the sidewall insulation ($55 \text{ }^\circ\text{C}$). Bottom insulation results in a higher panel temperature than in the only sidewall condition. Henceforth, in this experimental work, an ISPB still without insulation on improving the freshwater yield by varying the flow condition (m_f) has been carried out. The most important feature of the ISPB still is that it can produce power and freshwater.

Experimental setup

The schematic drawing and experimental arrangement of the proposed PISPB still is shown in Figs. 1 and 2, respectively. In this work, solar still basin made by steel is replaced by a PV panel. The dimensions of the system are 181 cm length, 92 cm breadth and 15 cm height. The sidewalls and the collector are made of a transparent glass.

Cotton thread is placed in between the PV cells which could absorb the flowing water for evaporation. Furthermore, continuous evaporation and absorption of water by the cotton thread decrease the PV cell temperature. A plastic control valve is fixed in between the storage tank and inlet pipe of the PISPB which could be used to vary the flow rate of saline water to the PISPB still basin. The input supply water is varied at different m_f such as 4.68, 7.56 and 10.08 kg h^{-1} , respectively. Hot water collected at the lower end of PISPB still is reused again and filled in the main storage tank for every one hour. During the operation of PISPB still, deposition of salts on the PV panel surface is a major issue, and every two weeks, it is cleaned using Windex crystal rain glass cleaner which could remove the salt deposition on the absorber plate. The glass cover, basin, panel, water and atmospheric temperatures were measured by temperature sensors. The condensed water through inner glass surface is collected at the end and accumulated in the distillate collector. The distillate collector is kept inclined so that the accumulated water gets collected in the calibrated jar for measurement.

The details of instruments used, parameters measured using the instruments, accuracy, range and % error produced by the instruments used for the present experimental investigation are tabulated in Table 1. The details of cost involved in fabricating the PISPB still are given in Table 2.

For different flow conditions (m_f) namely (1) 4.68, (2) 7.56 and (3) 10.08 kg h^{-1} , the entire experiments were conducted during the month of July 2019. The atmospheric conditions maintained during the experiments were almost similar, and the average solar radiation for the test days is

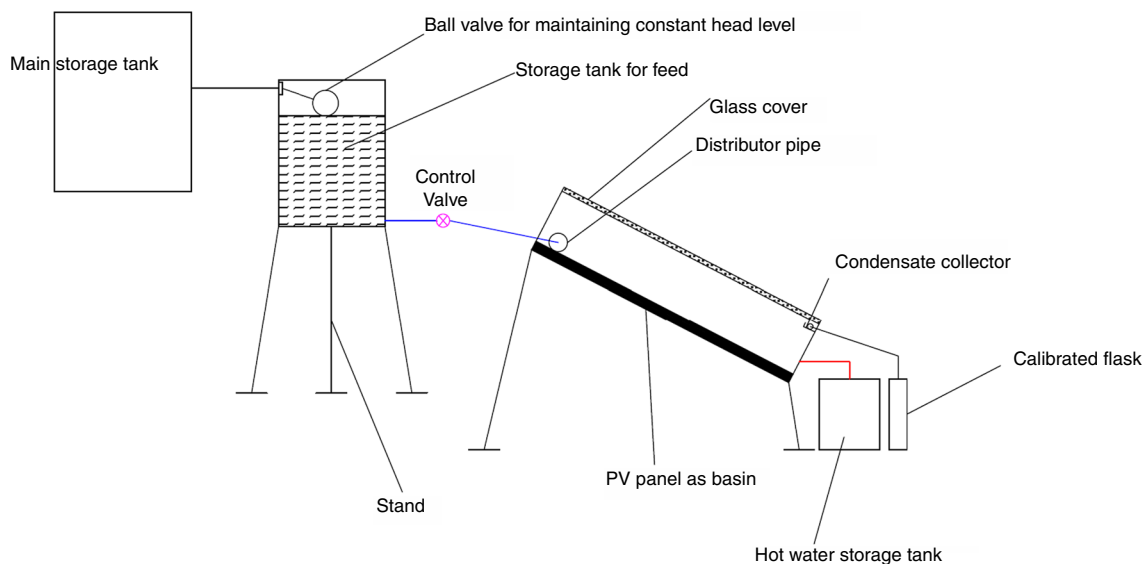


Fig. 1 Representational diagram of PISPB still without insulation



Fig. 2 Experimental setup of PISP still without insulation

measured as 694, 692, and 710 W m⁻² for 3.7.2017, 6.7.2017 and 12.7.2017, respectively.

Results and discussion

Hourly fluctuation of wind speed, solar intensity, atmospheric, glass, basin, water and panel temperature of the PISP still

Hourly variations of wind speed throughout the investigational day are plotted in Fig. 3a. The average wind speed throughout the investigational day is measured as 1.35, 1.67 and 1.76 m s⁻¹ for the flow rates of 4.68, 7.56 and 10.08 kg h⁻¹, respectively.

Hourly variations of the solar intensity, atmospheric, glass, basin, water and panel temperature of the PISP still at different *m_f* are drawn in Fig. 4a–c. From the graph, it is identified that solar intensity continuously increases during the forenoon session and attains its peak solar intensity during 13:00 Hrs, and the solar intensity values fall during

the afternoon. It is noted that the maximum solar intensity of 910, 930 and 960 W m⁻² is recorded on 3.7.2017, 6.7.2017 and 12.7.2017, respectively. The daily average solar radiation during the test dates is noted as 694, 692 and 710 W m⁻² for the flow conditions of (*m_f*) 4.68, 7.56 and 10.08 kg h⁻¹, respectively.

It is observed that atmospheric temperature also has trend similar to that of solar intensity, and its maximum value reaches up to 36, 35 and 36 °C obtained on 3.7.2017, 6.7.2017 and 12.7.2017, respectively, at 2 p.m. The average atmosphere temperature during the experimental day is between 32 and 33 °C.

The maximum temperature of 55, 54 and 52 °C in glass cover is recorded on 3.7.2017, 6.7.2017 and 12.7.2017, respectively. As a result of lower wind velocity, the collector external cover temperature of the PISP still increases. With a possible increase in the wind speed, results in reduced cover temperature as the convective heat transfer rate between the collector cover and ambient are higher which simultaneously increase the rate of condensation in the inner cover surface. The average glass cover temperature measured during the test days for corresponding wind velocity of 1.35, 1.67 and 1.98 m s⁻¹ is found as 48.23, 46.89 and 45.56 °C, respectively.

A linear increase in the basin temperature is observed, and the peak value is obtained during 14:00 Hrs and thereafter declined as the solar intensity reduces. The maximum attainable temperature by the basin of PISP still using different flow conditions of (*m_f*) 4.68, 7.56 and 10.08 kg h⁻¹ are 64, 57 and 53 °C, respectively. Average basin temperature of the PISP still for different flow conditions of (*m_f*) 4.68, 7.56 and 10.08 kg h⁻¹ is found as 50.33, 46.11 and 43.11 °C, respectively. With possible increase in the flow condition (*m_f*) from 4.68 to 7.56 kg h⁻¹, it is found that the average basin temperature drop by 9.15%, and with further increase in the flow conditions (*m_f*) from 7.56 to 10.08 kg h⁻¹, it is noted that there is a possible decrease in temperature of basin to about 16.75%. This is due to the interaction of higher flow conditions; the lower temperature water with higher temperature basin extracts the heat continuously as the retention time of water with basin is higher which simultaneously resulted in reduced temperature of basin.

Table 1 Measured parameters, accuracy, range and error limits for different measuring instruments

S. no.	Instruments	Measured parameter	Accuracy	Range	% error
1	Thermocouple	Temperature	± 1 °C	0–120 °C	0.5
2	Solar power meter	Solar intensity	± 2 W m ⁻²	0–2000 W m ⁻²	2.5
3	Anemometer	Wind speed	± 0.1 m s ⁻¹	0–10 m s ⁻¹	10
4	Measuring jar	Water mass	± 10 m L	0–1500 m L	10
5	Multimeter	Voltage and current	± 1 V ± 0.1 A	0–100 V 0–10 A	0.5 10

Table 2 Cost breakdowns for the PISBP still

S. no.	Materials	Unit cost/Rs.	Total cost/Rs.
1	Basin material (150 W PV panel)	Rs. 90/Watt	Rs. 13,500
2	Sidewalls and glass cover	Rs. 2000	Rs. 2000
3	Distillate collector	Rs. 200	Rs. 200
4	Basin and basin material	(A)	Rs. 15,700
4	Stand storage tank	Rs. 2000	Rs. 2000
5	Control valve	Rs. 200	Rs. 200
7	Labor cost	Rs. 300/h	Rs. 600
	Accessories and labor cost	(B)	Rs. 2800
	Total cost	(A + B)	Rs. 18,500

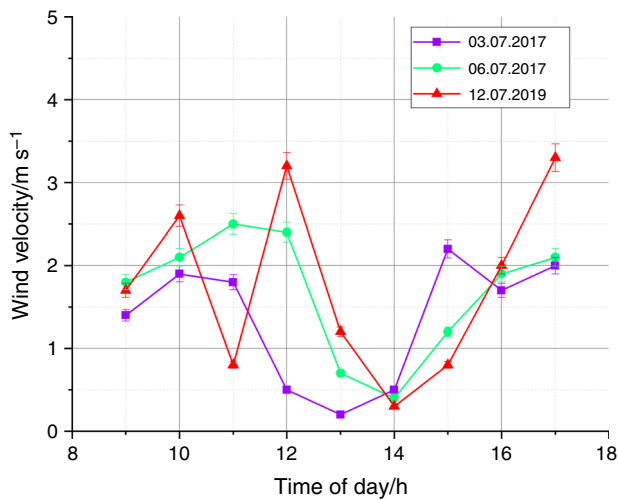


Fig. 3 Variations of wind speed with respect to time

From the obtained results of water temperature at different flow conditions, it is found that the maximum temperature of water is achieved during 14:00 Hrs as similar to the temperature of basin. The maximum recorded temperature of water temperature using different flow conditions of ISPB still is 65, 62 and 58 °C for flow conditions of 4.68, 7.56 and 10.08 kg h⁻¹, respectively. The average water temperature of the ISPB still is 53.22, 50.77 and 48.5 °C at *m_f* at 4.68, 7.56 and 10.08 kg h⁻¹, respectively. It is observed that there is a decrease of about 4.81% in the average water temperature, while the flow condition is increased from 4.68 to 7.56 kg h⁻¹ and similarly, there is a decrease of about 9.61% in the average water temperature while the flow conditions (*m_f*) from 7.56 to 10.08 kg h⁻¹. The reason for decrease in water temperature is, the contact time between the ISPB still basin and the saline water is reduced. When the ISPB still operates at minimum *m_f*, it extracts the maximum heat from the ISPB still basin which resulted in higher water temperature. An increase in *m_f* reduces the water temperature and consequently it produced the less productivity

It is seen that panel temperature reaches the maximal value of 53, 51 and 48 °C at the *m_f* at 4.68, 7.56 and 10.08 kg h⁻¹, respectively. The daily average panel temperature reaches 43.11, 40.55 and 37.88 °C at the *m_f* at 4.68, 7.56 and 10.08 kg h⁻¹, respectively. There is a fall in panel temperature when the *m_f* increases. It is found that when the *m_f* increases from 4.68 to 7.56 kg h⁻¹ and 4.68 to 10.08 kg s⁻¹, there are a 6.3 and 13.78% decreases in the panel temperature.

Influence of mass flow rate over internal heat transfer, cumulative yield, energy and exergy efficiency

On an hourly basis, the variations in evaporative heat transfer coefficient of PISPB still for different flow conditions are plotted in Fig. 5. The peak EHTC is observed nearly at 14:00 Hrs, and its value is 55.95, 48.46 and 43.27 W m⁻² K⁻¹ for the *m_f* at 4.68, 7.56 and 10.08 kg h⁻¹, respectively. The average EHTC of 25.75, 20.29 and 12.87 W m⁻² K⁻¹ is obtained at the *m_f* at 4.68, 7.56 and 10.08 kg h⁻¹, respectively. When the *m_f* increases from 4.68 to 7.56 kg h⁻¹ and 4.68 to 10.08 kg s⁻¹, there are 21.18 and 50% decreases in EHTC. An increase in the *m_f* reduces the EHTC because of reduces in saline water temperature. EHTC is inversely proportional to the temperature variation between the saline water and collector cover, solar intensity.

EHTC between water and glass is estimated using,

$$h_{e,w-g} = 16.273 \times 10^{-3} \times h_{c,w-g} \left[\frac{P_w - P_{gi}}{T_w - T_{gi}} \right] \tag{1}$$

CHTC between water and glass is estimated using,

$$h_{c,w-g} = 0.884 \left[(T_w - T_{gi}) + \frac{(P_w - P_{gi})(T_w + 273)}{(268.9 \times 10^{-3} - P_w)} \right] \tag{2}$$

Partial vapor pressure at water and inner surface of the glass is given by,

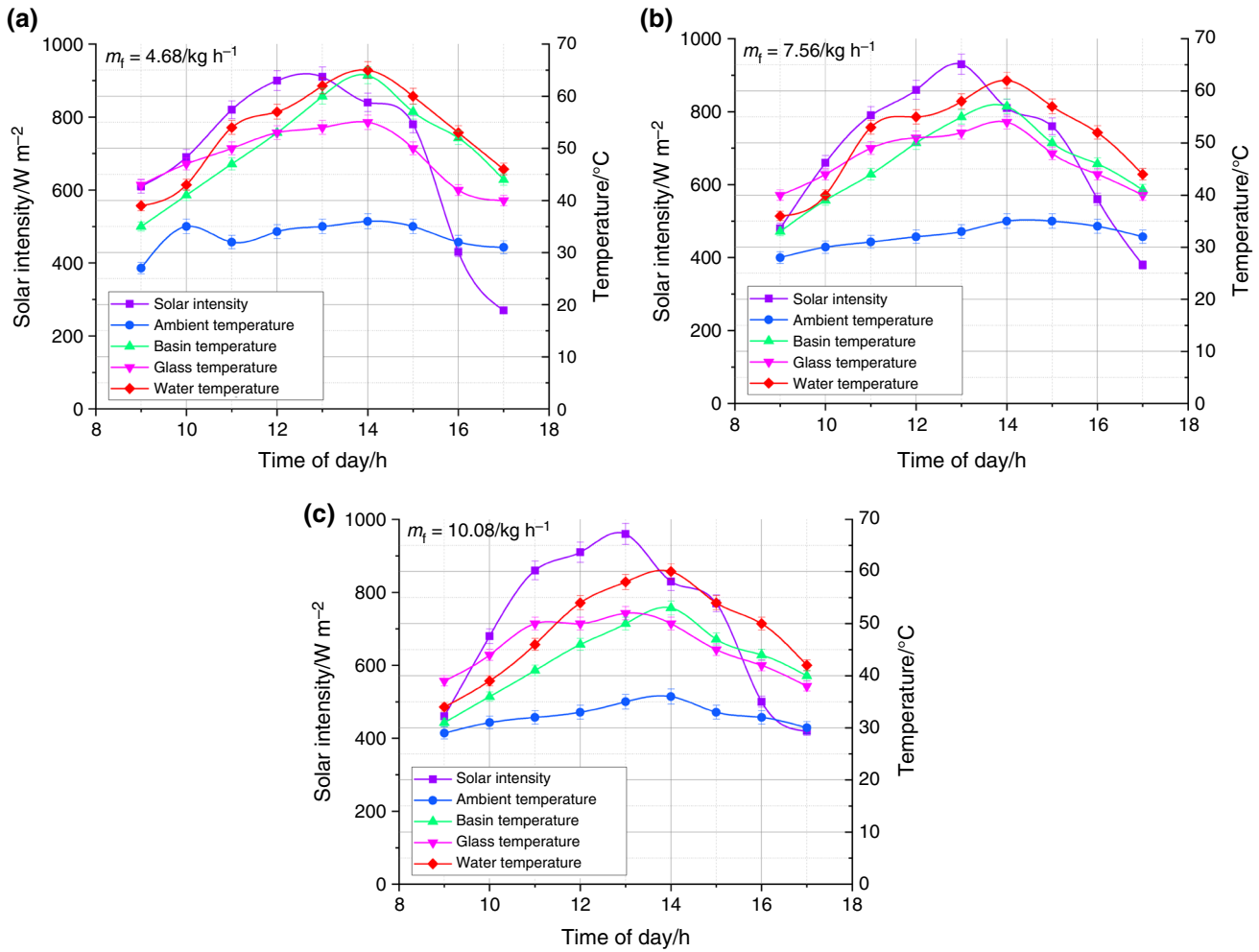


Fig. 4 Variations of solar irradiance, atmospheric, glass, water, basin and the panel temperature of the PISPB still

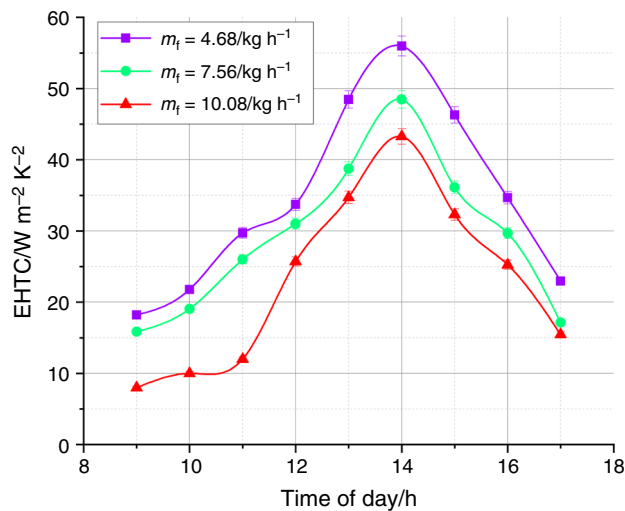


Fig. 5 Variations of EHTC for the ISPB still with respect to time

$$P_w = \exp\left(25.317 - \left(\frac{5144}{273 + T_w}\right)\right) \quad (3)$$

$$P_{gi} = \exp\left(25.317 - \left(\frac{5144}{273 + T_{gi}}\right)\right) \quad (4)$$

Variations of accumulated productivity for the PISPB still at different m_f are shown in Fig. 6. The maximum hourly productivity produced from the PISPB still is maximum at minimum flow condition (m_f). The maximum hourly productivity of 0.82, 0.61 and 0.45 kg is obtained at the m_f at 4.68, 7.56 and 10.08 $kg h^{-1}$, respectively. The daily productivity of 3.75, 2.7 and 1.6 kg is obtained at the m_f at 4.68, 7.56 and 10.08 $kg h^{-1}$, respectively. When the m_f increases from 4.68 to 7.56 $kg h^{-1}$ and 4.68 to 10.08 $kg s^{-1}$, there is a 28.16 and 55.48% decreases in daily yield.

The variation in hourly thermal efficiency of ISPB still under different flow conditions is plotted in Fig. 7. The maximum hourly thermal efficiency of 68.11, 47.77 and 34.64% is obtained for the m_f at 4.68, 7.56 and

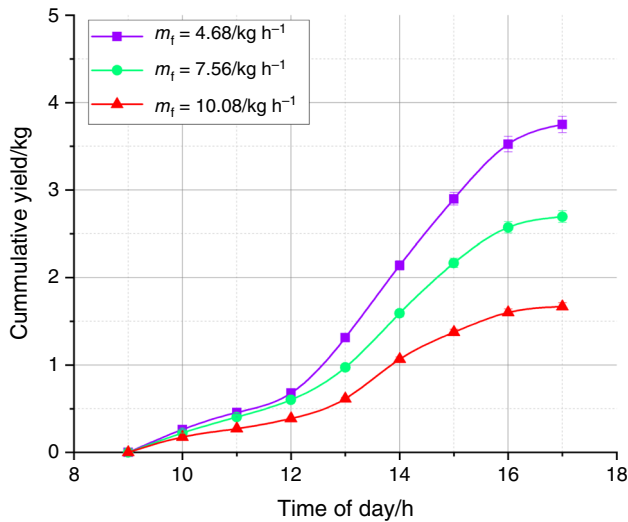


Fig. 6 Variations of accumulated productivity for the PISPB still with respect to time

10.08 kg h⁻¹, respectively. The daily thermal efficiency of 36.06, 25.56 and 16.95% is obtained for the m_f at 4.68, 7.56 and 10.08 kg h⁻¹, respectively. When the m_f increases from 4.68 to 7.56 kg h⁻¹ and 4.68 to 10.08 kg s⁻¹, there is a 29.11 and 53% decreases in thermal efficiency. The detailed summary of distilled water produced and efficiency of passive-type ISPB is shown in Table 3. The improvement in yield and efficiency is observed in the case of lower flow rates.

The thermal efficiency of the PISPB still is given by,

$$\eta_{\text{passive}} = \frac{\sum \dot{m}_{\text{ew}} L}{\sum I(t) A_s \times 3600} \times 100 \tag{5}$$

The variations of the exergy efficiency of the PISPB still at different flow condition (m_f) are plotted in Fig. 8. With

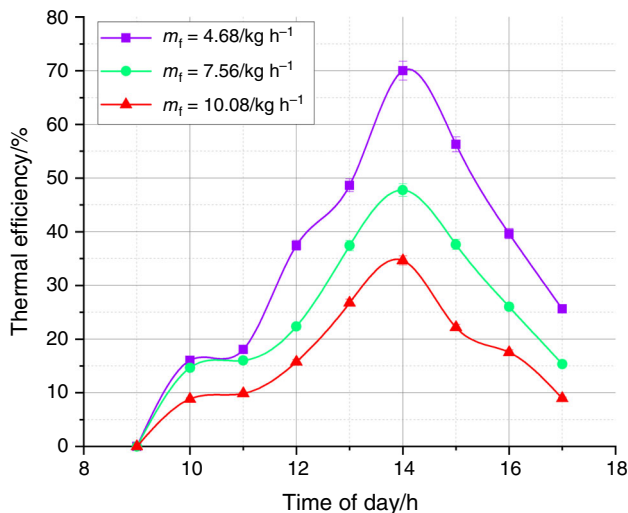


Fig. 7 Variations of thermal efficiency for the PISPB still with respect to time

the increase in solar intensity, the exergy efficiency increases and the peak is observed during 14:00 Hrs and thereafter declined as the solar intensity reduces. The maximum hourly exergy efficiency of 6.38, 4.43 and 2.77 is obtained for m_f at 4.68, 7.56 and 10.08 kg h⁻¹, respectively. The exergy efficiency of the PISPB still different flow condition (m_f) of 4.68, 7.56 and 10.08 kg h⁻¹ is found as 2.97, 1.91 and 1.01%, respectively. By increasing the rate of flow (m_f) from 4.68 to 7.56 and from 4.68 to 10.08 kg h⁻¹, exergy efficiency of the still decreases by 35.77 and 66.08%, respectively. It is decided that the exergy efficiency of the still is directly proportional to the distilled water produced from the PISPB still. Higher productivity results in higher exergy efficiency. In this work, an increase in the m_f results in less productivity, and hence it produced lower exergy efficiency.

The exergy efficacy of the PISPB still is calculated by,

$$\eta_{p,e} = \frac{e_{p,\text{out}}}{e_{p,\text{in}}} \tag{6}$$

The exergy output of the PISPB still is calculated by,

$$e_{p,\text{out}} = (m_d \times h_{fg}) \left(1 - \left[\frac{T_a + 273}{T_w + 273} \right] \right) \tag{7}$$

The exergy input of the PISPB still is calculated by,

$$e_{p,\text{in}} = (A \times I_t) \left[1 + \left(\frac{1}{3} \left[\frac{T_a + 273}{6000} \right]^4 - \frac{4}{3} \left[\frac{T_a + 273}{6000} \right] \right) \right] \tag{8}$$

Influence of mass flow rate over power production, electrical, thermal and exergy efficiency of photovoltaic panel

Variations of the solar panel power production from the PISPB still at different flow condition (m_f) are shown in Fig. 9. From Fig. 9, it is inferred that the power produced from the photovoltaic panel during the peak solar intensity period under corresponding flow condition of 4.68, 7.56 and 10.08 kg h⁻¹ is found as 72, 77.7 and 83.6 W. The average power generation from the PV panel is 50.25, 54.75 and 60.03 watts for the m_f at 4.68, 7.56 and 10.08 kg h⁻¹, respectively. With the continuous flow of water inside the inclined photovoltaic panel, the efficiency is improved at higher flow rate condition and the consolidated results are tabulated in Table 4. Due to the reduction in flow rate of water, the temperature of panel (basin) reduces which resulted in lower power produced. Similarly, the increase in flow rate of water resulted in reduced temperature of panel (basin) which increased the power production by photovoltaic panel. It is found that daily average panel temperature decreases up to 6.3% which in

Table 3 Improvements in productivity and the thermal and exergy efficiency of the PISPB still for different m_f

S. no.	Mass flow rate/kg h ⁻¹	Yield/kg		Thermal efficiency/%		Exergy efficiency/%	
		Actual	% increase	Actual	% increase	Actual	% increase
1	10.08	1.6	Reference	16.95	Reference	1.01	Reference
2	7.56	2.7	40.74	25.56	33.68	1.91	47.12
3	4.68	3.75	57.33	36.06	53	2.97	59.93

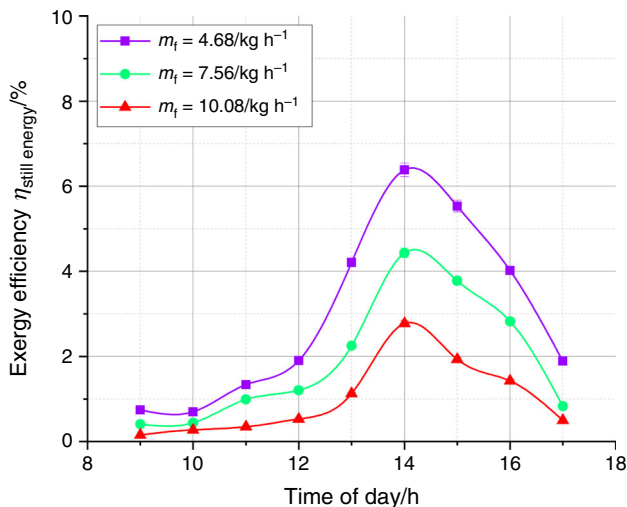


Fig. 8 Variations of exergy efficiency for an ISPB still with respect to time

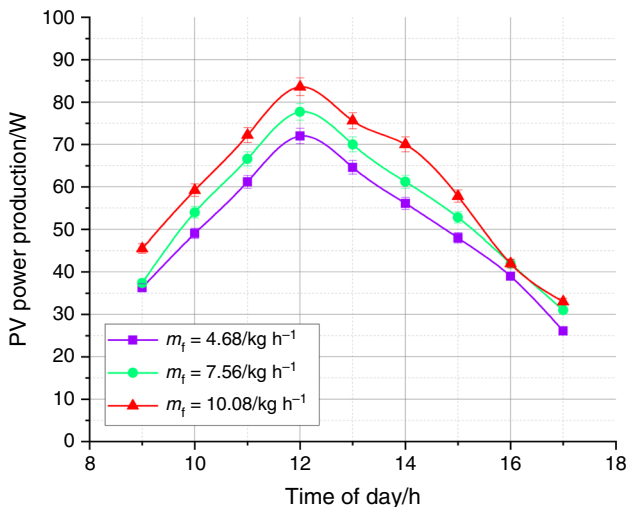


Fig. 9 Variations of the PV panel power generation for an ISPB still with respect to time

turn increases the power production and panel efficiency up to 8.2% and 8.66%, respectively. Similarly, a 13.78% decrease in panel temperature increases the power

production and panel efficiency up to 16.3% 13.81%, respectively.

Figure 10 shows the PV panel electrical and thermal efficiency of an ISPB still at different m_f . The efficiency of the PV panel reaches its maximum at 12 p.m., there after the efficiency decreased and reached a minimum at 3 p.m. Later 3 p.m., again the PV panel efficiency starts increasing. The maximum hourly PV panel electrical efficiency about 8.77% [$T_p = 47\text{ }^\circ\text{C}$, $I(t) = 900\text{ W m}^{-2}$], 10.04% [$T_p = 43\text{ }^\circ\text{C}$, $I(t) = 860\text{ W m}^{-2}$] and 10.32% [$T_p = 39\text{ }^\circ\text{C}$, $I(t) = 910\text{ W m}^{-2}$] is obtained at m_f at 4.68, 7.56 and 10.08 kg h⁻¹, respectively. From the above-mentioned results, it is clear that the PV panel efficiency does not only depend on the solar irradiance but also on the panel temperature. Considering the m_f data at 4.68 and 7.56 kg h⁻¹, in this case the deviation between the solar intensity and panel temperature is found to be 40 W m⁻² and 4 °C. Even though the panel receives a lesser solar intensity of 40 W m⁻², it yields 1.3% higher PV efficiency because of 4 °C drop-in panel temperature. At 3 p.m., the PV panel electrical efficiency reached its lower value of 6.93% [$T_p = 47\text{ }^\circ\text{C}$, $I(t) = 780\text{ W m}^{-2}$], 7.72% [$T_p = 45\text{ }^\circ\text{C}$, $I(t) = 760\text{ W m}^{-2}$] and 8.23% [$T_p = 43\text{ }^\circ\text{C}$, $I(t) = 770\text{ W m}^{-2}$] at m_f at 4.68, 7.56 and 10.08 kg h⁻¹, respectively. In this case, the highest $I(t) = 780\text{ W m}^{-2}$ produced the lowest PV panel efficiency of 6.93% and the lowest $T_p = 43\text{ }^\circ\text{C}$ produced the highest PV panel efficiency of 8.23%. After 3 p.m., the PV panel temperature starts increasing. At 5 p.m., the efficiency of 8.37% [$T_p = 39\text{ }^\circ\text{C}$, $I(t) = 420\text{ W m}^{-2}$], 8.61% [$T_p = 37\text{ }^\circ\text{C}$, $I(t) = 380\text{ W m}^{-2}$] and 9.55% [$T_p = 35\text{ }^\circ\text{C}$, $I(t) = 270\text{ W m}^{-2}$] is obtained for the m_f at 4.68, 7.56 and 10.08 kg h⁻¹, respectively.

The daily average PV panel efficiency of an ISPB still under m_f at 4.68, 7.56 and 10.08 kg h⁻¹ is 8.05, 8.81 and 9.44%, respectively. An increase in the m_f from 4.68 to 7.56 kg h⁻¹ results in decreases in the daily average PV panel temperature from 43.11 to 40.56 °C which enhances the PV panel efficiency from 8.05 to 8.81%. Similarly, further increase in m_f to 10.08 kg h⁻¹ results in reducing the daily average PV panel temperature to 37.89 °C which enhances the PV panel efficiency to 9.44%.

The solar panel electrical efficacy is estimated as [46–48],

Table 4 Improvements in the PV panel power generation and efficiency of the ISPB still by increasing the mass flow rate of water

S. no.	Mass flow rate/kg h ⁻¹	PV panel power/W		PV panel efficiency/%	
		Actual	% increase	Actual	% increase
1	4.68	50.25	Reference	8.05	Reference
2	7.56	54.75	8.22	8.81	8.63
3	10.08	60.03	16.3	9.34	13.81

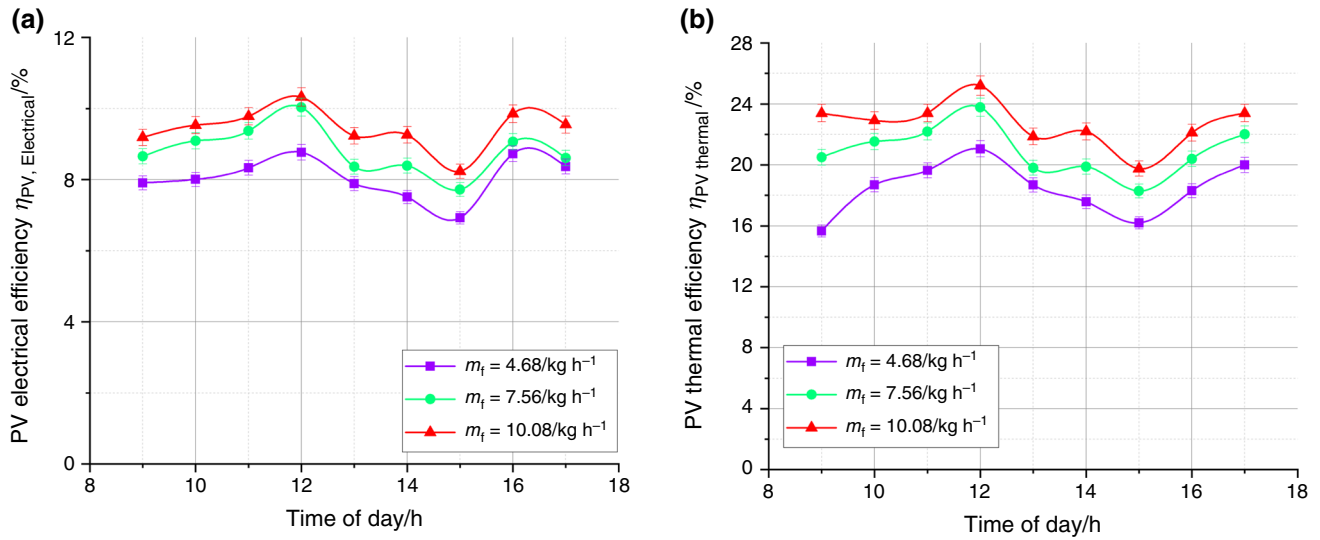


Fig. 10 Variations of **a** the PV panel electrical and **b** the thermal efficiency for an ISPB still with respect to time

$$\eta_{pv \text{ electrical}} = \frac{FF * V * I}{I_s(t) * A_s} \times 100\% \tag{9}$$

Thermal efficiency produced by the solar panel also has the same trend as the electrical efficiency of the PV panel because the thermal efficiency of the PV panel is obtained by just multiplying the denominator term of the electrical efficiency formula by conventional power plant electricity generation efficiency (0.38). This constant is used to find the thermal efficiency of the PV system.

The PV panel thermal efficiency is mathematically expressed as [46–48],

$$\eta_{pv \text{ thermal}} = \frac{FF * V_{oc} * I_{sc}}{0.38I_s(t) * A_s} \times 100\% \tag{10}$$

The variations of the PV panel exergy efficiency at different m_f are plotted in Fig. 11. It is observed that during lower solar irradiance, the exergy efficacy calculated for the photovoltaic panel is lower and the lowest exergy efficiency of 10.10, 10.51 and 11.21% and the highest exergy efficiency of 38.12, 40.30 and 41.43% under flow condition of (m_f) 4.68, 7.56 and 10.08 kg h⁻¹, respectively. The daily average exergy efficiency of the PV panel is found as 19.38, 20.58 and 21.16% at m_f at 4.68, 7.56 and 10.08 kg h⁻¹, respectively. It is found that increasing the m_f from 4.68 to 7.56 kg h⁻¹, and 4.68 to 10.08 kg h⁻¹

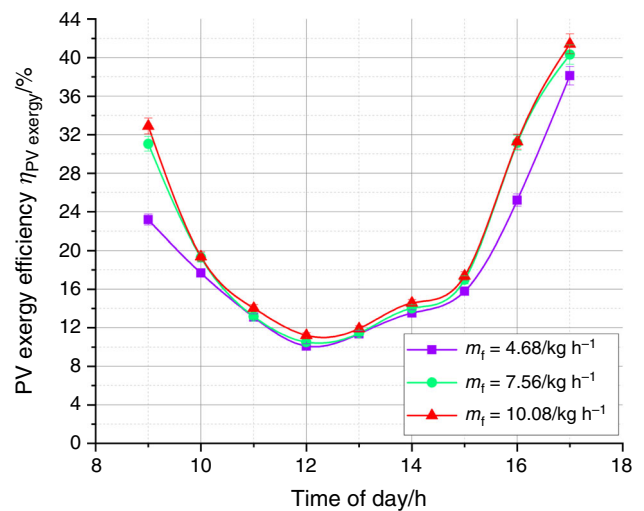


Fig. 11 Variations of the PV panel exergy efficiency for an ISPB still with respect to time

increases the PV panel exergy efficiency by about 5.83 and 8.42%, respectively.

The mathematical correlation for estimating the panel exergy efficiency is as follows [46–48],

$$\eta_{pv \text{ exergy}} = \frac{FF * V_{oc} * I_{sc} - VI}{0.933I_s(t) * A_s} \times 100\% \tag{11}$$

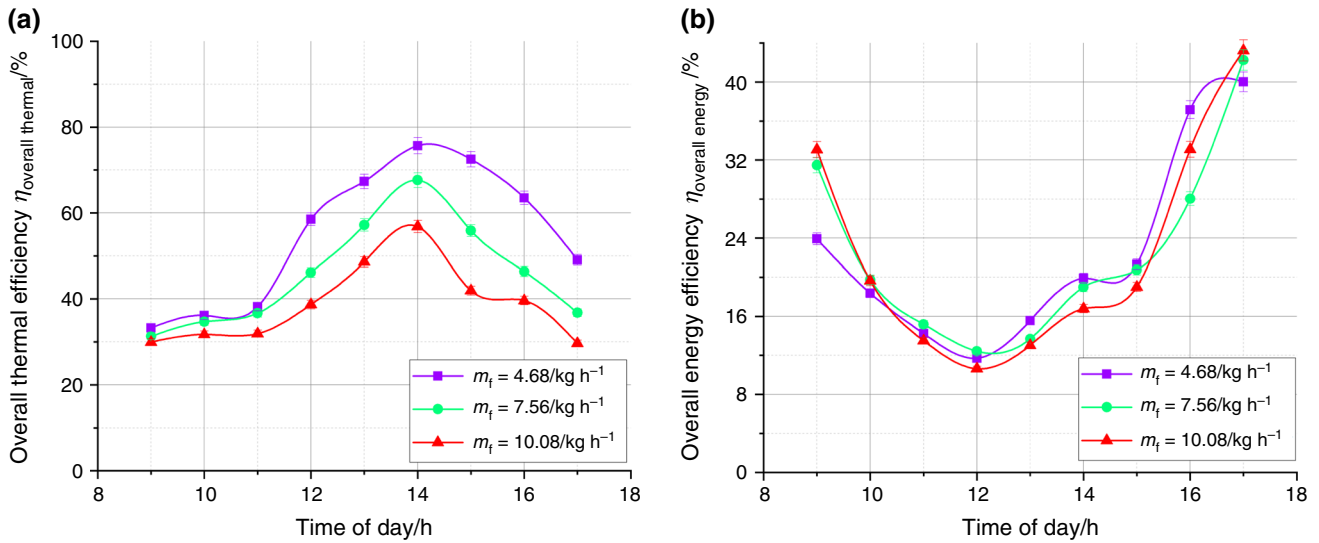


Fig. 12 Variations of the a overall thermal efficiency b overall exergy efficiency for an ISPB still with respect to time

Effect of mass flow rate on overall thermal and exergy efficiency

Figure 12a shows the hourly variations in system overall thermal efficiency (IPSB still and photovoltaic panel) of system for different flow conditions. It is observed that at minimum flow condition, the overall system efficiency is higher, whereas the efficiency decreases as the rate of flow by the water increases. On observing the overall thermal efficiency, the IPSB efficiency decreases at higher flow rates, whereas the photovoltaic panel thermal efficiency increases which as the fact of reduced panel temperature. The peak thermal efficiency during maximum solar intensity on PISPB still is found as 75.69, 67.66 and 56.84% for the flow conditions of (m_f) 4.68, 7.56 and 10.08 kg h⁻¹, respectively. Similarly, overall thermal efficiency of the system (IPSB still and photovoltaic panel) is found as 51.32, 44.59 and 43.68% for the flow conditions of (m_f) 4.68, 7.56 and 10.08 kg h⁻¹, respectively. It is concluded that there is a 13.12 and 14.88% decrease in the overall thermal efficiency of the system when the m_f increases from 4.68 to 7.56 kg h⁻¹ and 4.68 to 10.08 kg h⁻¹, respectively.

Based on the electrical output, area of collector, amount of distilled water collected and solar intensity, the overall thermal efficiency is estimated and it is mathematically expressed as [46–48],

$$\eta_{\text{overall P.thermal}} = \frac{m_{ew} * h_{fg}}{I_s(t) * A_s * 3600} \times 100\% + \frac{FF * V_{oc} * I_{sc} - VI}{0.933I_s(t) * A_s} \times 100\% \quad (12)$$

The overall exergy efficiency of the ISPB still for different flow conditions of water is plotted in Fig. 12b. Based on Eq. (12), the overall exergy efficiency of the system (PISPB) is calculated and estimated as 21.79, 22.85 and 22.79% for different flow conditions of 4.68, 7.56 and 10.08 kg h⁻¹, respectively. It is also observed that the daily exergy efficiency of the photovoltaic panel increases with increased flow conditions, while the exergy efficiency decreases with increased flow condition. The reduced exergy efficiency and increased panel efficiency resulted in equaling the overall exergy efficiency for all flow conditions.

The overall exergy efficiency of the PISPB still is calculated by [46–48],

$$\eta_{\text{overall P.exergy}} = \frac{(m_d * h_{fg}) \left(1 - \left[\frac{T_a + 273}{T_w + 273}\right]\right)}{(A_s * I_t) \left[1 + \left(\frac{1}{3} \left[\frac{T_a + 273}{6000}\right]^4 - \frac{4}{3} \left[\frac{T_a + 273}{6000}\right]\right)\right]} + \frac{FF * V_{oc} * I_{sc} - VI}{0.933I_s(t) * A_s} \times 100\% \quad (13)$$

Conclusions

The outcome of modifying mass flow rate on the PISPB still was experimentally analyzed, and it was stated that increasing the m_f results in a decrease in water and panel temperature. Water temperature is directly proportional to the ISPB still productivity, whereas panel temperature is inversely proportional to the PV panel production and efficiency. The daily productivity from the ISPB still is 3.7, 2.7 and 1.6 kg for the mass flow rate of 4.68, 7.56 and

10.08 kg h⁻¹, respectively. The daily thermal efficiency of an ISPB still is found as 36.06, 25.56 and 16.95% for the respective flow conditions of 4.68, 7.56 and 10.08 kg h⁻¹, whereas the daily panel efficiency for the same flow conditions is found as 8.05, 8.81 and 9.34%. When m_f is increased from 4.68 to 7.56, the daily yield and thermal efficiency of the ISPB still decrease by about 28.16 and 29.11%, respectively, while the power produced and efficiency of the photovoltaic panel increase to about 8.2 and 8.66%, respectively. When m_f increased from 4.68 to 10.08 kg h⁻¹, there is a decrease of about 55.48 and 53% in the ISPB still productivity and thermal efficiency, respectively, and the power produced and efficiency increase by 16.3 and 13.81%, respectively. From the experimental studies, it is concluded that increasing the m_f results in lower freshwater production and higher panel efficiency.

References

1. Omara ZM, Abdullah AS, Dakrory T. Improving the productivity of solar still by using water fan and wind turbine. *Sol Energy*. 2017;147:181–8.
2. Kabeel AE, Sathyamurthy R, El-Agouz SA, Manokar AM, El-Said EM. Experimental studies on inclined PV panel solar still with cover cooling and PCM. *J Therm Anal Calorim*. 2019;3:191–7.
3. Kabeel AE, Abdelgaied M, Sathyamurthy R. A comprehensive investigation of the optimization cooling technique for improving the performance of PV module with reflectors under Egyptian conditions. *Sol Energy*. 2019;186:257–63.
4. Sathyamurthy R, Kabeel AE, El-Agouz ES, Rufus D, Panchal H, Arunkumar T, Manokar AM, Winston DGP. Experimental investigation on the effect of MgO and TiO₂ nanoparticles in stepped solar still. *Int J Energy Res*. 2019;43(8):3295–305.
5. Kabeel AE, Manokar AM, Sathyamurthy R, Winston DP, El-Agouz SA, Chamkha AJ. A review on different design modifications employed in inclined solar still for enhancing the productivity. *J Sol Energy Eng*. 2019;141(3):031007.
6. Panchal H, Sathyamurthy R, Kabeel AE, El-Agouz SA, Rufus D, Arunkumar T, Manokar AM, Winston DP, Sharma A, Thakar N, Sadasivuni KK. Annual performance analysis of adding different nanofluids in stepped solar still. *J Therm Anal Calorim*. 2019. <https://doi.org/10.1007/s10973-019-08346-x>.
7. Sathyamurthy R, El-Agouz E. Experimental analysis and exergy efficiency of a conventional solar still with Fresnel lens and energy storage material. *Heat Transf Asian Res*. 2019;48(3):885–95.
8. Manokar AM, Winston DP, Sathyamurthy R, Kabeel AE, Prasath AR. Experimental investigation on pyramid solar still in passive and active mode. *Heat Mass Transf*. 2019;55(4):1045–58.
9. Sharshir SW, Ellakany YM, Algazzar AM, Elsheikh AH, Elkaadem MR, Edreis EM, et al. A mini review of techniques used to improve the tubular solar still performance for solar water desalination. *Process Saf Environ Prot*. 2019;124:204–12.
10. Madhu B, Balasubramanian E, Kabeel AE, Sathyamurthy R, El-Agouz ES, Muthu Manokar A. Experimental investigation on the effect of photovoltaic panel partially and fully submerged in water. *Heat Transf Asian Res*. 2019. <https://doi.org/10.1002/htj.21453>.
11. Khechekhouché A, Benhaoua B, Manokar AM, Kabeel AE, Sathyamurthy R. Exploitation of an insulated air chamber as a glazed cover of a conventional solar still. *Heat Transf Asian Res*. 2019;48(5):1563–74.
12. Madhu B, Balasubramanian E, Kabeel AE, El-Agouz SA, Manokar AM, Prakash N, Sathyamurthy R. Experimental investigation on the effect of sensible heat energy storage in an inclined solar still with baffles. *Desalin Water Treat*. 2018;116:49–56.
13. Manokar AM, Vimala M, Sathyamurthy R, Kabeel AE, Winston DP, Chamkha AJ. Enhancement of potable water production from an inclined photovoltaic panel absorber solar still by integrating with flat-plate collector. *Environ Dev Sustain*. 2019. <https://doi.org/10.1007/s10668-019-00376-7>.
14. Manokar AM, Vimala M, Winston DP, Sathyamurthy R, Kabeel AE. Effect of insulation on energy and exergy effectiveness of a solar photovoltaic panel incorporated inclined solar still—an experimental investigation. In: Kumar A, Prakash O, editors. *Solar desalination technology*. Singapore: Springer; 2019. p. 275–92.
15. Kabeel AE, Taamneh Y, Sathyamurthy R, Naveen Kumar P, Manokar AM, Arunkumar T. Experimental study on conventional solar still integrated with inclined solar still under different water depth. *Heat Transf Asian Res*. 2019;48(1):100–14.
16. Manokar AM, Taamneh Y, Kabeel AE, Sathyamurthy R, Winston DP, Chamkha AJ. Review of different methods employed in pyramidal solar still desalination to augment the yield of freshwater. *Desalin Water Treat*. 2018;136:20–30.
17. Panchal H, Mevada D, Sathyamurthy R. The requirement of various methods to improve distillate output of solar still: a review. *Int J Ambient Energy*. 2018. <https://doi.org/10.1080/01430750.2018.1542630>.
18. Kabeel AE, El-Agouz SA, Sathyamurthy R, Arunkumar T. Augmenting the productivity of solar still using jute cloth knitted with sand heat energy storage. *Desalination*. 2018;443:122–9.
19. Singh DB, Tiwari GN. Energy, exergy and cost analyses of N identical evacuated tubular collectors integrated basin type solar stills: a comparative study. *Sol Energy*. 2017;155:829–46.
20. Singh DB, Tiwari GN. Enhancement in energy metrics of double slope solar still by incorporating N identical PVT collectors. *Sol Energy*. 2017;143:142–61.
21. Singh DB, Tiwari GN. Performance analysis of basin type solar stills integrated with N identical photovoltaic thermal (PVT) compound parabolic concentrator (CPC) collectors: a comparative study. *Sol Energy*. 2017;142:144–58.
22. Singh DB, Tiwari GN, Al-Helal IM, Dwivedi VK, Yadav JK. Effect of energy matrices on life cycle cost analysis of passive solar stills. *Sol Energy*. 2016;134:9–22.
23. Manokar AM, Prince Winston D, Kabeel AE, El-Agouz SA, Sathyamurthy R, Arunkumar T, Madhu B, Ahsan A. Integrated PV/T solar still—a mini-review. *Desalination*. 2017. <https://doi.org/10.1016/j.desal.2017.04.022>.
24. Kabeel AE, Abdelgaied M. Observational study of modified solar still coupled with oil serpentine loop from cylindrical parabolic concentrator and phase changing material under basin. *Sol Energy*. 2017;144:71–8.
25. El-Agouz SA, El-Samadony YAF, Kabeel AE. Performance evaluation of a continuous flow inclined solar still desalination system. *Energy Convers Manag*. 2015;101:606–15.
26. Aybar HS. Mathematical modeling of an inclined solar water distillation system. *Desalination*. 2006;190:63–70.
27. Aybar HS, Egelioglu F, Atikol U. An experimental study on an inclined solar distillation system. *Desalination*. 2005;180:285–9.
28. Sharon H, Reddy KS, Krithika D, Philip L. Experimental performance investigation of tilted solar still with basin and wick for

- distillate quality and enviro-economic aspects. *Desalination*. 2017;410:30–54.
29. Yeh HM, Chen ZF. Experimental studies on wick-type, double-effect solar distillers with air flow through the second-effect unit. *Energy*. 1992;17(3):269–73.
 30. Yeh HM, Chen ZF. Energy balances in wick-type double-effect solar distillers with air flow through the second-effect unit. *Energy*. 1992;17(12):1239–47.
 31. Sathyamurthy R, Samuel DH, Nagarajan PK. Theoretical analysis of inclined solar still with baffle plates for improving the fresh water yield. *Process Saf Environ Prot*. 2016;101:93–107.
 32. Nagarajan PK, El-Agouz SA, Harris Samuel DG, Edwin M, Madhu B, Sathyamurthy R, Bharathwaaj R. Analysis of an inclined solar still with baffles for improving the yield of fresh water. *Process Saf Environ Prot*. 2017;105:326–37.
 33. El-Agouz SA. Experimental investigation of stepped solar still with continuous water circulation. *Energy Convers Manag*. 2014;86:186–93.
 34. Omara ZM, Kabeel AE, Younes MM. Enhancing the stepped solar still performance using internal reflectors. *Desalination*. 2013;314:67–72.
 35. Omara ZM, Kabeel AE, Younes MM. Enhancing the stepped solar still performance using internal and external reflectors. *Energy Convers Manag*. 2014;78:876–81.
 36. Sodha MS, Kumar A, Tiwari GN, Tyagi RC. Simple multiple wick solar still: analysis and performance. *Sol Energy*. 1981;26(2):127–31.
 37. Sathyamurthy R, Nagarajan PK, El-Agouz SA, Jaiganesh V, Khanna PS. Experimental investigation on a semi-circular trough-absorber solar still with baffles for fresh water production. *Energy Convers Manag*. 2015;97:235–42.
 38. Naveen Kumar P, Harris Samuel DG, Nagarajan PK, Sathyamurthy R. Theoretical analysis of a triangular pyramid solar still integrated to an inclined solar still with baffles. *Int J Ambient Energy*. 2016;34:597–603.
 39. Kumar PN, Manokar AM, Madhu B, Kabeel AE, Arunkumar T, Panchal H, Sathyamurthy R. Experimental investigation on the effect of water mass in triangular pyramid solar still integrated to inclined solar still. *Groundw Sustain Dev*. 2017;5:229–34.
 40. Panchal H, Taamneh Y, Sathyamurthy R, Kabeel AE, El-Agouz SA, Kumar PN, et al. Economic and Exergy investigation of triangular pyramid solar still integrated to inclined solar still with baffles. *Int J Ambient Energy*. 2019;40:571–6.
 41. Murugavel KK, Anburaj P, Hanson RS, Elango T. Progresses in inclined type solar stills. *Renew Sustain Energy Rev*. 2013;20:364–77.
 42. Kaviti AK, Yadav A, Shukla A. Inclined solar still designs: a review. *Renew Sustain Energy Rev*. 2016;54:429–51.
 43. Farshchi TF, Mohammad D, Hamid M, Kiyanoosh R. Effect of water flow rate on internal heat and mass transfer and daily productivity of a weir-type cascade solar still. *Desalination*. 2010;260:239–47.
 44. Manokar AM, Prince Winston D, Kabeel AE, Sathyamurthy R. Sustainable fresh water and power production by integrating PV panel in inclined solar still. *J Clean Prod*. 2018. <https://doi.org/10.1016/j.jclepro.2017.11.140>.
 45. Manokar AM, Winston DP, Mondol JD, Sathyamurthy R, Kabeel AE, Panchal H. Comparative study of an inclined solar panel basin solar still in passive and active mode. *Sol Energy*. 2018;169:206–16.
 46. Singh DB, Yadav JK, Dwivedi VK, Kumar S, Tiwari GN, Al-Helal IM. Experimental studies of active solar still integrated with two hybrid PVT collectors. *Sol Energy*. 2016;130:207–23.
 47. Singh DB, Al-Helal IM. Energy metrics analysis of N identical evacuated tubular collectors integrated double slope solar still. *Desalination*. 2018;432:10–22.
 48. Singh DB. Improving the performance of single slope solar still by including N identical PVT collectors. *Appl Therm Eng*. 2018;131:167–79.

Publisher's Note Springer Nature remains neutral with regard to jurisdictional claims in published maps and institutional affiliations.